Nonlinear Self-Tuning Control for Soft Landing of an Electromechanical Valve Actuator

Katherine Peterson[†], Anna Stefanopoulou[†], Yan Wang[‡], Mohammad Haghgooie[‡]

[†]Mechanical Engineering Department, Univ of Michigan, Ann Arbor

[‡]Scientific Research Laboratory, Ford Motor Company, Dearborn

Abstract: Electromechanical valve actuators (EVA) can be used for electronic control of the engine valves. Their operation requires fast and precise motion of an armature between two stiff springs and two voltage-controlled electromagnets. Low contact velocities or "soft landing" of the actuator on the solenoid faces and between the actuator and the valve is also necessary in order to maintain similar noise and wear levels with conventional camshaft-driven engines. We analyze the control difficulties, review the actuator model and extend our previous work by introducing impact dynamics. We then design a self-tuning nonlinear controller using extremum seeking that achieves impact velocities below 0.1 m/s and maximum transition time of 4.0 ms. *Copyright ©2002 IFAC*

Keywords: Nonlinear Control; Averaging; Stability; Automotive; Electromagnetic Actuation

1 Introduction

Electromagnetic (EM) actuation provides reliable means and a popular alternative to hydraulic or pneumatic actuation for implementing control systems. It is a natural connection between electrical circuits and mechanical systems. All electromagnetic actuators work upon the same basic principle. By inducing current in a coil of wire, the actuator gives rise to a magnetic force, which is then used to affect the movement of some physical component. Such systems have two distinct advantages; the applied force is non-contacting, and often the response of the electromagnet is significantly faster then the dynamics of the system being controlled.

Due to their usefulness, electromechanical actuator using electromagnets are found in a wide range of applications. Of particular interest are the applications with translational (linear) motion, large induced forces, and contacts between the activating and the actuating parts. These characteristics provide critical functionality in emerging technological areas such as bio-engineering and telecommunication routing devices. In bio-engineering an EM actuator controls intra-ventricular balloons to simulate a beating heart [2] and implantable drug delivery systems [10]. Optical switches [13] used in controlling telecommunication traffic are activated using EM or electrostatic actuation. In mature technological areas such as process and automotive industry EM actuation enables new designs. For example, electromagnets have been introduced for flow and distributed mixing control via throttling during material processing [3]. In automotive applications they are used in fuel injectors [19], fast actuating valves such as idle speed bypass and wastegate, and potentially valvetrain control as shown in Fig. 1.

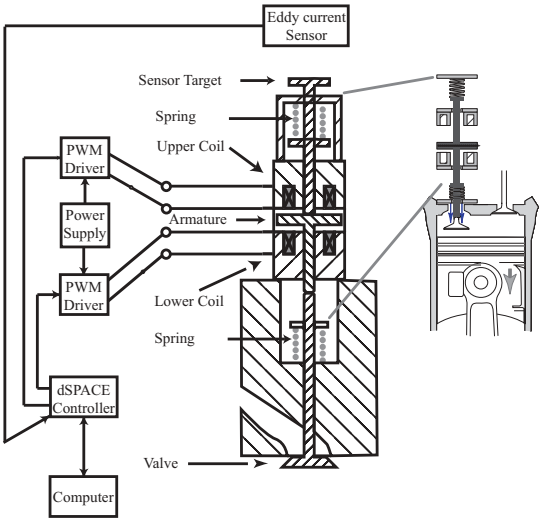

Figure 1: Electromechanical valve actuator and experimental setup.

Electronic control of engine valves and fully variable valve timing can be achieved with EM actuation. Extensive effort has been and is being made in the design of actuator mechanisms at research and devel-

[†] Support is provided by the National Science Foundation under contract NSF-ECS-0049025 and Ford Motor Company through a 2001 University Research Project.

opment laboratories throughout the world. A search performed in Feb 2002 with keywords *camless*, *engine*, *valve*, *control*, *solenoid* for patents filled in Europe, United States and Japan resulted 303 relevant patents; 37 of which were filled after Sep 2001. The focus of this paper is the dynamical analysis and control design of the EVA mechanism shown in Fig. 1 in order to ensure precise motion control, fast transitions and low contact velocities. These requirements are universal in EM actuation independently of the application area and the operating environment.

2 Electromechanical Valve Actuator

The EMV actuator studied in this paper is shown in Fig. 1. The actuator governs the opening/closing of the valve through the forcing of a set of springs and electromagnets. A typical opening/closing cycle is shown in Fig. 2. Initially the armature is held in the closed position by the upper magnetic coil, causing the spring on that side to be more compressed than the opposing spring. At time t_{rc} the release command is given and the voltage across the upper magnetic coil is reduced to zero. The difference in the spring force drives the armature across the 8 mm gap, thereby causing the valve to open. A catching voltage is applied to the lower magnetic coil to ensure the armature is caught. Once the armature has been captured, a holding voltage is applied to hold the valve open. At time t_{ro} the process is reversed in order to close the valve. For more information on the functionality of the system the reader is referred to [7].

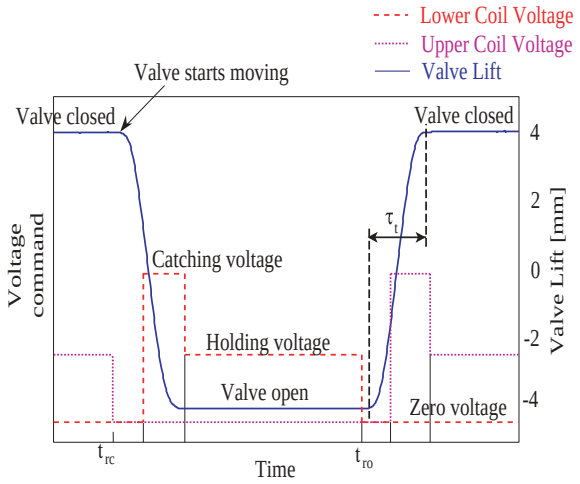

Figure 2: Typical valve opening/closing cycle.

The experimental setup consists of the following components; Electromechanical Valve Actuator, Eddy Current Sensor, 2 PWM Drivers, 200 Volt Power Supply, and a Dspace 1103 processing board. The eddy current sensor is mounted on the rear of the actuator and measures the armature displacement, which is sampled by the Dspace processor at 20 kHz. Based on the displacement and the control algorithm, the Dspace processing board regulates the PWM frequency to each of the PWM drivers to achieve the desired performance.

Before the actuator can be implemented in production vehicles, impact velocities less than 0.1 m/s and transition times of less than 4 ms need to be achieved. The first specification is required to avoid excessive noise and wear on the system, while the second is to avoid variability in trapped mass and collision with the piston.

Due to non-elastic collision, the armature will bounce before coming to rest against the catching coil. As such, we define the impact velocity to be the largest velocity of the armature when it is in contact with the catching coil. Typically this corresponds to the first collision. As the change in trapped mass is negligible after the armature has completed 98% of its travel, the transition time is defined as the time from release to when the armature is 98% closed/open.

Various control methodologies have been proposed to achieve the desired performance. Specifically, optimal control with no position sensor are used in [1], iterative learning in [4], linear observer-based control in [14], and repetitive methodology in [17]. Here, a self-tunning nonlinear feedback using extremum seeking is used to achieve the desired functionality. Initial results of this methodology were presented in [15].

3 Nonlinear Model

In [20] a theoretical model for the EMV actuator is presented and validated against experimental results. The system consists of four states, namely, armature position (z in mm), armature velocity (v in m/s), upper coil current (i_u, in A) and lower coil current (i_l in A). To achieve fast release a reverse polarity voltage technique, described in [20], is used to quickly drive the holding current to zero. Therefore the current in the releasing coil has little influence over the motion of the armature, and as such the system can be reduced from four states to three. The three state model is defined as: catching coil current (i, in A), distance from the catching coil (z, in mm), and armature velocity (v in m/s). The resulting equations of motion are:

$$\frac{di}{dt} = \frac{V_c - ri + \chi_1(i,z)\,v}{\chi_2(z)} \tag{3.1}$$

$$\frac{dz}{dt} = 1000v \tag{3.2}$$

$$\frac{dv}{dt} = \frac{1}{m}\left(-F_{mag}(i,z) + k_s(4-z) - bv + N\right)$$

where the catching coil voltage is denoted by V_c in V, the resistance r in Ω, the system mass m in kg, the spring stiffness k_s in N/mm, the damping coefficient b in Ns/m, the magnetic force due to the catching

coil F_{mag} in N, the back-EMF $\chi_1 v$ in V, and the inductance χ_2 in H. Neglecting saturation effects (see [20] for the exact model), the functions χ_1, χ_2, and F_{mag} are given by

$$\chi_1(i,z) = \frac{2k_a i}{(k_b+z)^2} \quad (3.3)$$

$$\chi_2(z) = \frac{2k_a}{1000(k_b+z)} \quad (3.4)$$

$$F_{mag}(i,z) = \frac{k_a i^2}{(k_b+z)^2} \quad (3.5)$$

where k_a and k_b are constants.

The force N is the normal force acting between the armature and catching coil during impact:

$$N = \begin{cases} \text{if } z \neq 0, & 0 \\ \text{if } z = 0, & \begin{cases} \text{if } v = 0, & F_{mag}(i,0) - 4k_s \\ \text{if } v \neq 0, & \begin{cases} \text{if } v < 0, & \delta \\ \text{if } v > 0 & 0 \end{cases} \end{cases} \end{cases}$$

where δ is an impulse function calibrated to give $v^+ = ev^-$, where v^+ is the velocity just after impact and v^- is the velocity just before impact. The parameter $e < 1$ is chosen based on experimental data and represents the loss of kinetic energy due to the plastic collision.

A comparison of the model response to experimental data is shown in Fig. 3 and the detailed behavior during impact is shown in Fig. 4. The data is generated by using a 120 V catching voltage applied to the lower coil 1.5 ms after the armature is released from the upper coil.

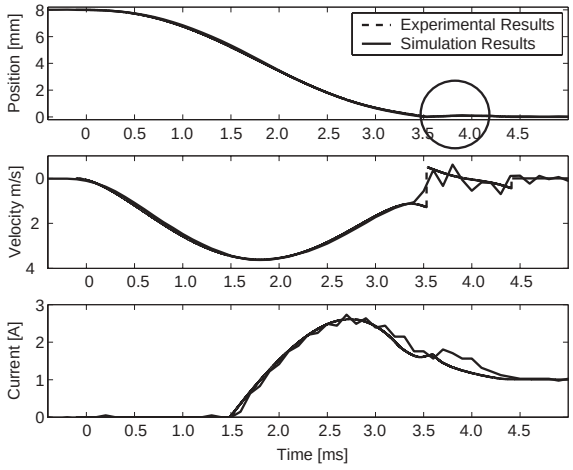

Figure 3: Comparison of the model to experimental data. See Fig 4 for an enlarged view of the encircled region

The model is written compactly as

$$\frac{dx}{dt} = f(x, V_c), \quad x = \begin{bmatrix} i & z & v \end{bmatrix}^T \quad (3.6)$$

The addition of the normal force not only adds impact dynamics, but explicitly shows the multiple equilibria

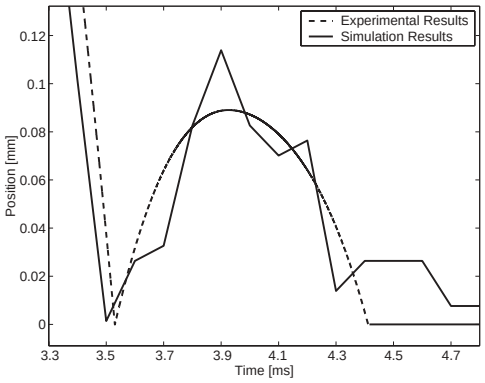

Figure 4: Enlarged view of the encircled region of Fig. 3

of the system at the contact point. The system is at equilibrium for the set of states and inputs

$$x_e = \{[i, z, v] \mid i \geq i_e, z = 0, v = 0\}$$

$$i_e = \{i \mid F_{mag}(i,0) = 4k_s\}, \; V_c = \frac{i}{r}.$$

A controller which drives the current to a value near i_e runs the risk of failing to stabilize the armature against the catching coil due to bouncing and/or other disturbances. On the other hand, a large holding current will increase the power consumption of the actuator reducing, and potentially eliminating, the projected fuel economy benefits of variable valve timing. A combined design-optimization study needs to be performed to rigorously address this question in the future.

4 Control Difficulties

The system suffers from low control authority over the armature position from the voltage input throughout the executed motion. The underlying reasons are dynamic during small gaps and static during large gaps. Specifically, during small gaps the low control authority arises from the decreased inductance combined with the increased back-EMF that drives the current to zero exceedingly fast. During large gaps the magnetic force is not strong enough to balance the spring force. These phenomena need to be understood in order to design a successful controller.

Assuming saturation effects are negligible, substitution of (3.3) and (3.4) into (3.1) yields;

$$\frac{di}{dt} = 1000\left(\frac{(V_c - ri)(k_b+z)}{2k_a} + \frac{iv}{(k_b+z)}\right).$$

Which is a first order approximation of the current dynamics since it neglects saturation affects. Note that $k_b \ll 1$ and z is approaching zero. Let us replace the term $k_b + z$ with the small parameter $\varepsilon = k_b + z$, resulting in

$$\frac{di}{dt} = 1000\left(\frac{(V_c - ri)\varepsilon}{2k_a} + \frac{iv}{\varepsilon}\right) \quad (4.1)$$

Two observations should be made from (4.1). First, the input voltage is being multiplied by ε, therefore very near the catching coil, the voltage cannot easily affect the current dynamics. Second if we multiply through by ε we see that the current dynamics become singularly perturbed near the catching coil. For $z > 1$ mm these affects aren't present as ε is greater than 1.

Similar to the above result, since $k_b \ll 1$ Eqn. (3.5) shows that the magnetic force drops off very rapidly as the armature moves away from the magnetic coil. For distances greater than approximately 1 mm from the catching coil the spring force dominates the system response as it is much greater than the magnetic force. Despite this, it is necessary to apply voltage to the catching coil while the armature is not near it. If voltage is not applied to the system until the armature is close to the catching coil, it will be extremely difficult to raise the current because of the back-EMF. It is much easier to raise the current before the system becomes singularly perturbed, and then apply large inputs near the end of the transition to overcome the effects of the changing back-EMF and inductance seen in equation (4.1).

5 Nonlinear Controller

Equation (4.1) shows the sever limitations of linear control methodologies for the EMV actuator. In a linear controller the input voltage is proportional to the error (i.e. $V_c = Kz$) exacerbating the decrease of the influence of the input voltage as z approaches zero. Thus large values of the gain, K, will be required to overcome the changing current dynamics. This can, and does lead to actuator saturation [14]. Moreover, it leads to small voltage inputs near the catching coil, potentially creating problems with bouncing.

To overcome the changing current dynamics and reduced control authority we propose the use of a nonlinear controller of the form

$$V_c = \frac{K_1}{\gamma + z} v + \frac{K_2}{\beta + z}. \tag{5.1}$$

The control input is inversely proportional to the distance from the catching coil, thereby alleviating the affect of the decreasing influence of the voltage on the current dynamics. The parameters K_1, K_2, γ, and β are used to tune the controller to achieve the desired performance. The position is measured with an eddy current sensor and a nonlinear observer designed in [14] is used to estimate velocity.

Since the current is not driven near the minimum equilibrium value, the magnetic force will remain larger than the spring force for small bounces. Thereby eliminating the potential loss of the armature due to bouncing.

Experimental results are shown in Fig. 5 and Table 1.

While the nonlinear controller does experience actuator saturation, it does so only at the very end of the transition. The nonlinear controller achieves a mean impact velocity of 0.16 m/s and transition time of 3.23 ms.

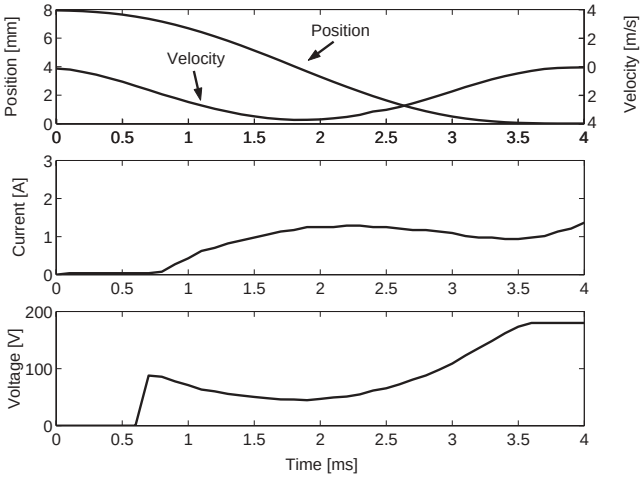

Figure 5: Experimental results achieved by using the nonlinear controller.

Table 1: Statistical results for the nonlinear controller.

	Transition Time	Impact Velocity
Mean	3.23 ms	0.16 m/s
σ	0.04 ms	0.08 m/s
Max	3.3 ms	0.32 m/s
Min	3.2 ms	0.05 m/s

6 Extremum Seeking Control

By applying a tuning algorithm from cycle to cycle it is possible to improve the performance of the actuator and adjust the controller parameters to account for changes in the system due to environmental variations.

Here, we apply an extremum seeking controller through the use of sinusoidal excitations [5] in order to tune the nonlinear feedback. An overview and proof [8] of this technique is repeated here for convenience. The proof relies on the theorem of averaging [6], which states that given a system $\frac{dx}{dt} = \varepsilon f(t, x, \varepsilon)$, $\varepsilon > 0$ where $f(t, x, \varepsilon)$ is sufficiently smooth and T-periodic in t, then

$$||x(t, \varepsilon) - x_{av}(t, \varepsilon)|| = O(\varepsilon)$$

where

$$\begin{aligned} \frac{dx_{av}}{dt} &= \varepsilon f_{av}(x) \text{ and} \\ f_{av}(x) &= \frac{1}{T} \int_0^T f(\tau, x, 0)\, d\tau. \end{aligned}$$

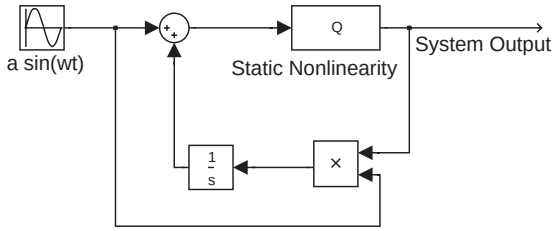

Figure 6: Extremum seeking feedback as applied to a static nonlinearity.

Stated qualitatively, a time varying periodic system can be approximated by the time invariant system derived from integrating the original system over a single period. If the resulting time invariant system is stable about an equilibrium, the time varying periodic system will converge to a periodic orbit about the same equilibrium.

The dynamics of the extremum seeking feedback applied to the static nonlinearity shown in Fig. 6 can be written as:

$$\frac{dx}{dt} = Q\left[x + a\sin(\omega t)\right] a\sin(\omega t)\,.$$

Let $\tau = \omega t$ and define $\widetilde{x}(\tau) = x\left(\frac{\tau}{\omega}\right)$, therefore

$$\frac{d\widetilde{x}}{d\tau} = \varepsilon Q\left[\widetilde{x} + a\sin(\tau)\right] a\sin(\tau)$$

where $\varepsilon = \frac{1}{\omega}$. Let Q be given by the Taylor series expansion

$$\begin{aligned} Q\left[\widetilde{x} + a\sin(\tau)\right] &= Q(\widetilde{x}) + \frac{\partial Q}{\partial \widetilde{x}}(\widetilde{x})\, a\sin(\tau) \\ &+ \frac{1}{2!}\frac{\partial^2 Q}{\partial \widetilde{x}^2}(\widetilde{x})\, a^2\sin^2(\tau) \end{aligned}$$

Applying the theorem of averaging we find

$$\frac{d\widetilde{x}_{av}}{d\tau} = \frac{a^2}{\varepsilon}\left(\frac{1}{2\pi}\int_0^{2\pi}\sin^2(\tau)\,d\tau\right)\frac{\partial Q}{\partial \widetilde{x}}(\widetilde{x}_{av})$$

where the equilibrium points are the local extremum of Q, and are stable if and only if $\left.\frac{\partial^2 Q}{\partial x^2}\right|_{x=x_e} < 0$, which occurs when x_e is a local maximum of Q.

Therefore by the theorem of averaging the system output will converge to a periodic orbit about a local maximum. By an identical proof it can be shown that the output is driven to a periodic orbit about a local minimum when the integrator in the feedback is multiplied by -1. For an overview of extremum seeking theory and methodologies the reader is referred to [16].

The EMV actuator and nonlinear feedback can be treated as a static nonlinearity if it is discretized with an appropriate sampling rate. If the sampling frequency is set equal to the frequency of the valve transitions, the extremum seeking feedback becomes

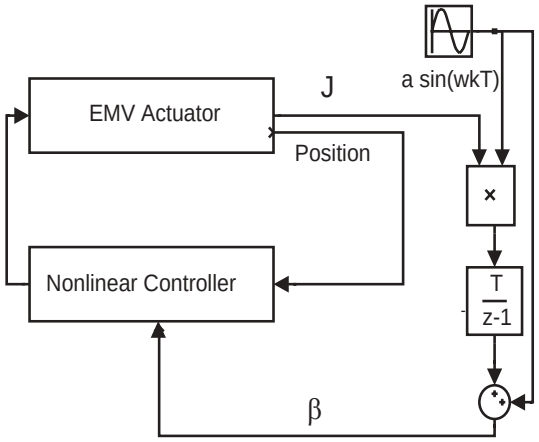

Figure 7: Extremum seeking feedback as applied to the EMV actuator.

oblivious to the EMV actuator dynamics. Next, the parameter β is selected as the input and the impact velocity, v_I, as the output. Therefore, from the perspective of the extremum seeking feedback the dynamic nonlinear system of the EMV actuator has been converted into a static nonlinear mapping from the parameter β to the impact velocity, v_I. The final setup is shown in Fig. 7.

Measuring the actual impact velocity is avoided by selecting a sensor whose output increases with increasing impact velocity, and decreases with decreasing impact velocity. Thus when the sensor output is minimized, the impact velocity is also minimized. In our experiment a small microphone is used to record the sound caused by the impact and the extremum seeking control is set to maximize the function $J = -(S_{min} - S_{meas})^2$. Where S_{min} is the desired sound level, and S_{meas} is the measured sound level. Note that S_{min} needs to be carefully set to a non-zero value otherwise the extremum seeking control will minimize the sound intensity by avoiding any contact which is obviously not desired. The output function can be generated by a variety of other sensors that relate to the impact velocity such as accelerometers, load washers, and knock sensors.

To test the extremum seeking control the feedback is initialized at a non-optimal value of β and allowed to run, the results are shown in Figs. 8-9. Initially the feedback achieves an impact velocity of approximately 0.4 m/s. After 40 iterations the extremum seeking control has reduced the velocity to a mean of approximately 0.08 m/s.

7 Conclusion and Future Work

The EMV actuator presents an interesting and challenging control design problem. The controller must achieve stringent performance requirements for soft and fast landing (impact velocities below 0.1 m/s and transition time smaller than 4.0 ms). The input-to-

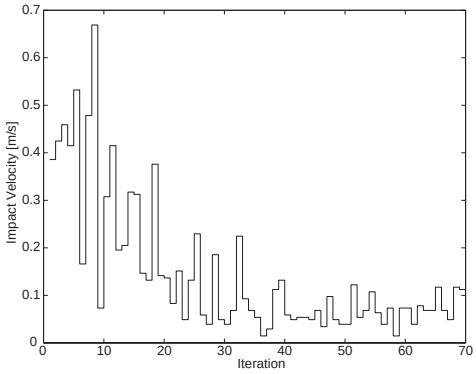

Figure 8: The impact velocity at each iteration.

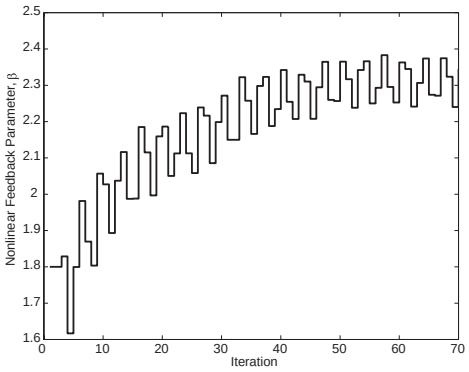

Figure 9: The parameter β of the nonlinear feedback at each iteration.

output behavior is nonlinear with low control authority for a combination of reasons that once understood a practical control solution arises.

Future work will investigate extending the extremum seeking control for multi-parameter tuning. The authors of [9] have shown that it is possible to simultaneously tune several parameters in order to minimize/maximize a single output. Hopefully by tuning all the parameters in the nonlinear feedback the extremum seeking control can further improve the performance and better adapt to a larger set of disturbances.

References

[1] Butzmann S., Melbert J., and Koch A., "Sensorless Control of Electromagnetic Actuators for Variable Valve Train," SAE Paper No. 2000-01-1225.

[2] Craver M. et. al., "Design of an Electromechanical Pump System for Training in Bleading Heart Cardiac Surgery," IEEE Proc Southeast Conference 2002.

[3] Gerber H., "Basis for the electromagnetic Throttling of Steel", 1997 IEEE Industry Applications 30th IAS IAS Annual Meeting.

[4] Hoffmann W., Stefanopoulou A., "Iterative Learning Control of Electromechanical Camless Valve Actuator," Proceedings American Control Conference, pp.2860-2866, June 2001.

[5] Jacobs 0., Shering G., "Design of a Single-Input Sinusoidal-Perturbation Extremum-Control System," Proceedings IEE, vol 115, pp212-217, 1968

[6] Khalil, *Nonlinear Systems*, Prentice Hall, 2^{nd} Ed., 1996.

[7] Kreuter P., Heuser P., and Schebitz M., "Strategies to Improve SI-Engine Performance by Means of Variable Intake Lift, Timing and Duration", SAE Paper No. 920449 , 1992.

[8] Krstic M., Wang H.H., "Stability of Extremum Seeking Feedback for General Nonlinear Dynamic Systems," Automatica, vol. 36, pp595-601, 2000.

[9] Krstic M., Ariyur K., "Analysis and Design of Multivariable Extremum Seeking," Proceedings American Control Conference, pp.2903-2908, May 2002

[10] Li C., Mantell S., Polla D., "Design and Simulation of an Implantable Medical Drug Delivery System Using Microelectromechanical Systems Technology," Sensors-and-Actuators-A-(Physical). vol.A94, no.1-2; 31 Oct. 2001; p.117-25.

[11] Lindlau J. D., Knospe C. R., "Feedback Linearization of an Active Magnetic Bearing with Voltage Control," IEEE Transactions on Control Systems Technology. vol.10, no.1; Jan. 2002; p.21-31.

[12] Mathews R. B., "Electromagnetic Control Device," United States Patent 2,769,943, August 22, 1949.

[13] Nonaka K. and Baillieul J., "Open Loop Robust Vibrational Stabilization of a Two Wire System Inside the Snap-Through Instability Region," Proc. IEEE Conference on Decision and Control. vol.2, pp. 1334-41, 2001, Orlando, FL, USA.

[14] Peterson K., Stefanopoulou A., Haghgooie M., Megli T. "Output Observer Based Feedback for Soft Landing of Electromechanical Camless Valvetrain Actuator", Proceedings of American Control Conference, pp. 1413-1418, May 2002.

[15] Stefanopoulou A., "Control of Electromechanical Actuators: Valves Tapping in Rhythm," Mohammed Dahleh Symposium, Feb. 2002, University of California, Santa Barbara.

[16] Stenby J., "Extremum Control Systems – An area for adaptive Control?" Proceedings of Joint Automatic Control, WA2-A, 1980.

[17] Tai C., Stubbs A., Tsao T.C., "Modeling and Controller Design of an Electromagnetic Engine Valve," Proceedings of American Control Conference, pp. 2890-2895, June 2001.

[18] Theobald M., Lequesne B., and Henry R., "Control of Engine Load via Electromagnetic Valve Actuators", SAE 940816.

[19] Ueda S., Mori Y., Iwanari E., Oguma Y. and Minoura Y., "Development of a New Injector in Gasoline Direct Injection System," SAE 2000-01-1046

[20] Wang Y., Stefanopoulou A., Peterson K., Megli T., Haghgooie M., "Modeling and Control of Electromechanical Valve Actuator," SAE 2002-01-1106